TRANSFER PROCESSES IN THE BATH OF HIGH AMPERAGE ALUMINIUM REDUCTION CELL

Andrey Zavadyak, Peter Polyakov, Andrey Yasinskiy, Iliya Puzanov, Yuri Mikhalev, Sergey Shakhrai, Nikita Sharypov, Olga Yushkova, Andrey Polyakov

Abstract

Bath of the aluminum reduction cell (as a cell itself) is a dissipative system. Important parameters of its welfare among others are: proper volume, shape, potential distribution in the anode-cathode space (ACS), direction and value of the electrolyte velocity. Using indicator ($SrCl_2$) introduction, volume of the electrolyte V is determined. Derivation $\partial V/\partial I = 10$ dm^3/kA is found. Bath velocity (2-15 cm/s) and its direction using thermographic and hydrodynamic methods are ascertained. Velocities distribution is given.

Keywords: bath velocity, bath direction, bath volume, indicator

1 Introduction

The increase in amperage due to natural engineering aspirations, common sense and economic considerations is accompanied by a decrease in the volume of the electrolyte (per kA of current) due to an increase in the volume occupied by anodes, reduction of the anode-cathode distance (ACD) and a decrease in the volume of the channels between anodes. In some cases, these circumstances lead to diseases of the subsystems of the cell, namely of the anode and the electrolyte, in particular, to:

1. The nonuniform distribution of the oxygen ion concentration $C_{O^{2-}}$ in ACD and in the channels caused by the retarded transfer rate of the O^{2-} ion;
2. Uneven current distribution on the anode bottom;
3. As a consequence - to the formation of anode deformations (spikes, mushrooms, etc.).

It is clear that the diseases entail a worsening of KPI: a reduction in current efficiency, an increase in the specific energy and carbon consumption, an increase in labor force and deterioration in the environmental background.

The problem of the alumina concentration distribution and transfer of O^{2-} ions in the ACD has been investigated to some extent by many experts [1-15]. In Russia in the 1970s, in particular, it was shown that the concentration of alumina in the bath, depending on the coordinates, can differ by 2% [1-2]. The value of the bath volume V_b introduced into the ACD which is equal to the bath volume leaving ACD with bubble was estimated. The ratio V_b/V_g was ≈ 0.015 where V_g – is the gas volume [3]. Welch and co-workers noted that the difficulty of mass transfer increases with increasing capacity of the cell [5]. Norwegian experts have shown that increasing the productivity due to the increase in the amperage (and current density) requires knowledge of the alumina flux values feeding each anode and the alumina concentration as a function of the coordinates and time [6, 7].

Unfortunately, the correct solution of the equations of continuity, convective diffusion, momentum and energy conservation under conditions of a two-phase gas-electrolyte flow complicated by the uncertainty of the boundary conditions (ignorance of the anode angles, dust, different lifetime of each anode, the shape of the metal-electrolyte interface, etc.) in order to find the concentration of the O^{2-} ion as a function of the coordinates and time is not possible, and therefore experiments on cells that determine the volume of the bath, its direction and velocity, which makes it possible to achieve a uniform current distribution along the bottom of each anode, seems to be the most reliable way to improve hydrodynamics and associated electrolysis KPI.

2 Experiments

2.1 Volume of bath

The experiments were carried out on high amperage cells. A well-known method of indicators [12] was used, in which anhydrous strontium chloride served as an indicator is used. To determine the concentration of the Sr^{2+} ion, an X-ray fluorescence method with a sensitivity of 0.0035 wt.% Sr^{2+} was used.

The weight of the loaded $SrCl_2$ was 3.2 kg. Anhydrous strontium chloride was loaded into 6 places with the help of a steel tray, which provided the dissolution of the $SrCl_2$ samples in the bath.

The dependence of the strontium ion concentration C (wt.%) on time was found to become stationary in 180 min. after loading.

In this case, it is obvious

$$C = \frac{m}{m^*} \cdot 100, \tag{1}$$

where m – is the mass of Sr^{2+} in the lot, m^* - is the mass of the bath.

As $m^*=V \cdot \rho$, where V – is the volume of the bath, ρ – is the density of the bath, we have

$$V = \frac{m \cdot 100}{C \cdot \rho_T} \tag{2}$$

In equation (2)

$$\rho_T = 2{,}088 - 0{,}00088 \cdot (t - 1000) \tag{3}$$

The temperature of the bath of 6 cells was in the range from 955 to 960 ºC.

Masses and volumes of bathes are presented in Table 1.

Table 1 – Bath masses and volumes in the cells

No of cell	$C_{Sr^{2+}}$a, wt.%	Mass, kg	Volume, m^3
1	0.0112	9.384	4.571
2	0.0110	9.555	4.654
3	0.0108	9.731	4.741
4	0.0117	8.983	4.376
5	0.0096	10.948	5.333
6	0.0120	8.758	4.267

Average ratio $\alpha=V/I$ from measured V and I was ≈ 8.8 dm^3/kA. The relatively small volume of bath with respect to alumina consumed was found to be β = 1386 dm^3/(kg Al_2O_3·h), small values of α and β require increased attention to alumina feeding operation.

2.2 Direction of bath flow

To determine the direction of the bath movement, the device shown in Fig. 1 was implemented. It includes a blade 1, a U-shaped rod 2, a conical holder 3, a holding plate 4, a direction indicator 5, a fixing screw 6. All parts were made of stainless steel. The prototype of the developed device was a portable blade velocity meter, proposed by Potocnik et al. [16].

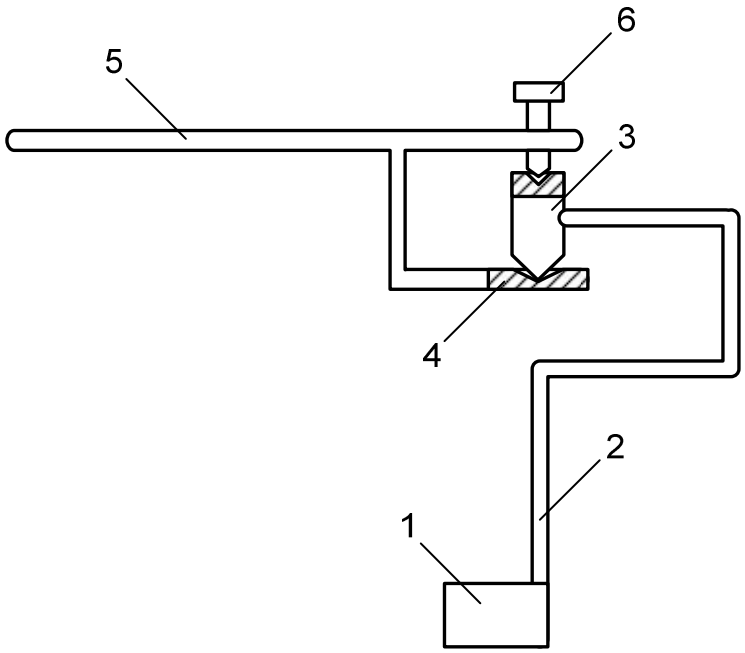

Fig. 1 - Device for measuring the direction of the bath flow

Blade 1 was immersed in the electrolyte in such a way that its upper edge was at the same level with the anode bottom, and the lower one - in the ACD with a blade height of 25 mm. The measurement at each point was made several times. The average directions of the electrolyte movement on eight cells are shown in Fig. 2.

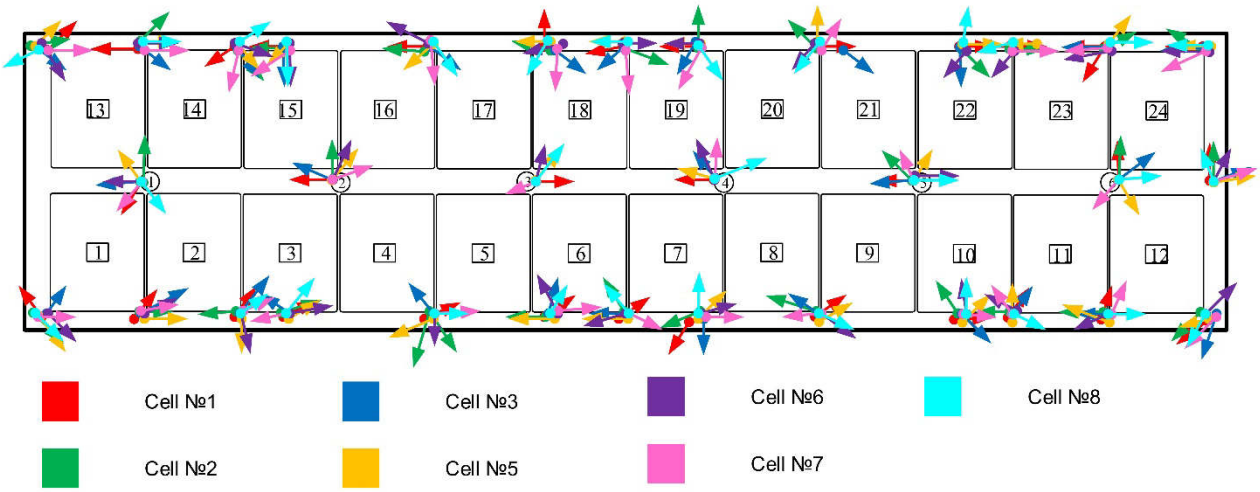

Fig. 2 – Results direction of measurements in the bath of eight cells

2.3 Velocity of bath flow

The velocity of the bath movement was determined by the velocity of alumina delivery to control points in which the direction of its movement was previously determined. To do this, thermocouples were installed in these points in a protective case made of steel with a wall thickness of 1 mm that were connected to the data collection system SPA-MVA-8, followed by the output and recording of measurement results on a PC.

To exclude the effect of alumina from nearby feeders on the bath velocity measurement, they were switched off at the time of measurement.

The delivery time was determined as the difference between the moment of loading of alumina by the feeder and the instant of the temperature drop at the control point [17].

The distance from the control point to the point of loading of alumina was determined by the Makita LD100P laser range finder (the measuring range is 0.05 ... 100 m, the accuracy of the measurements at a distance of up to 10 m equals ±1.5 mm).

The bath velocity was measured for one cell at key points around feeders No. 3 and No. 6 (Fig. 3). When measuring the movement velocity near the feeder 3 feeders 2 and 4 were disconnected, and in the case of measuring the movement velocity in the feeder 6 area feeders 4 and 5 were stopped. The rest of the feeders operated normally.

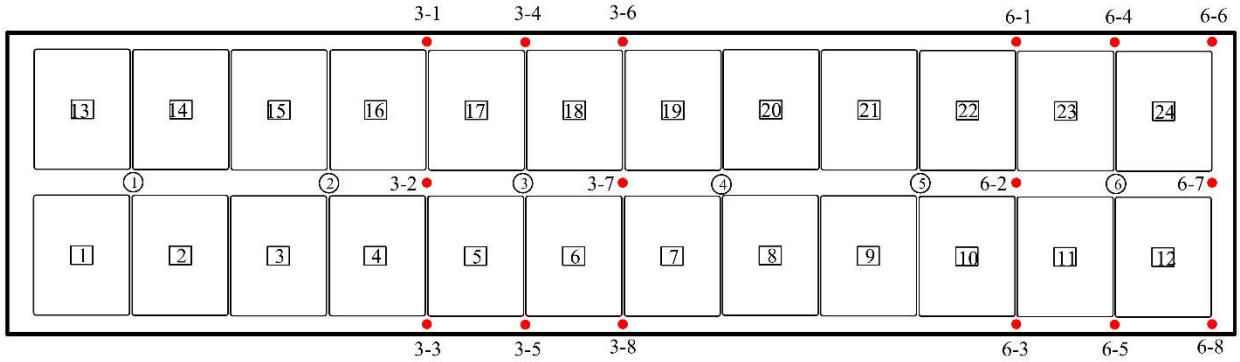

Fig. 3 - Measuring points (indicated in red) of the bath velocity (feeder areas 3 and 6)

For each feeder, the measurement was carried out for 30 minutes, the obtained velocities at the corresponding control points are shown in Table 2.

Table 2 - Bath velocities at the respective points of measurement

No of feeder	No of point	S, cm	V, cm/s	No of feeder	No of point	S, cm	V, cm/s
6	6-1	240	16,0	3	3-1	240	18,0
6	6-2	158	19,8	3	3-2	158	18,1
6	6-3	240	19,2	3	3-3	240	16,1
6	6-4	203	9,6	3	3-4	203	25,4
6	6-5	203	22,5	3	3-5	203	10,7
6	6-6	240	16,1	3	3-6	240	17,7
6	6-7	158	13,1	3	3-7	158	9,7
6	6-8	240	18,7	3	3-8	240	11,5

The average bath velocity was 16.4 cm/s, the standard deviation is 4.5 cm/s.

As a result of the bath movement direction measurements in 7 cells (Fig. 2), it can be noted:

– the preferential bath flow in the areas of the ledge-anode near the risers is directed from the side; the bath flow in the zones between the risers is directed into the ledge;

– at the corner points of the cell the flow is directed along the side channel of the bath from the duct end to the tap end;

– at the points of the end feeders (1 and 6), the bath flow is directed to the nearest end and to the side channels of the cell (this and previous results are consistent with the results of [16, 18]);

– at the points of the central feeders (2-4), the bath flow is directed along the current, i.e. to the downstream side;

Differences between the directions of bath flow in cells can be due to several reasons. The first of these is the age of the slotted anodes used. In the case of an “old” anode, there are no slots, and the bubble flow direction changes the

direction of the bath flow into the ACD [8, 19]. Nevertheless, there are areas where the bath direction does not depend on the age of the anodes.

The second reason may be the location of the cell inside the smelter, or rather the order of the cell relative to the other (whether the cell is first or the last), the magnetic fields in these cells are different from the fields of other cells, which leads to a change in the direction of the metal movement and, as a consequence, to a change in the bath flow, especially in areas where the metal velocities are high. This fact is of great importance in high-current electrolysis cells, working with small ACD. The studied seven cells were connected consequently side-by-side in the potline with the cell#4 being removed. The effect of the position of a cell in the potline on the bath movement direction is not obvious because of the age of the anode giving significant variation.

The average bath velocity as a function of coordinates is presented in Fig. 4.

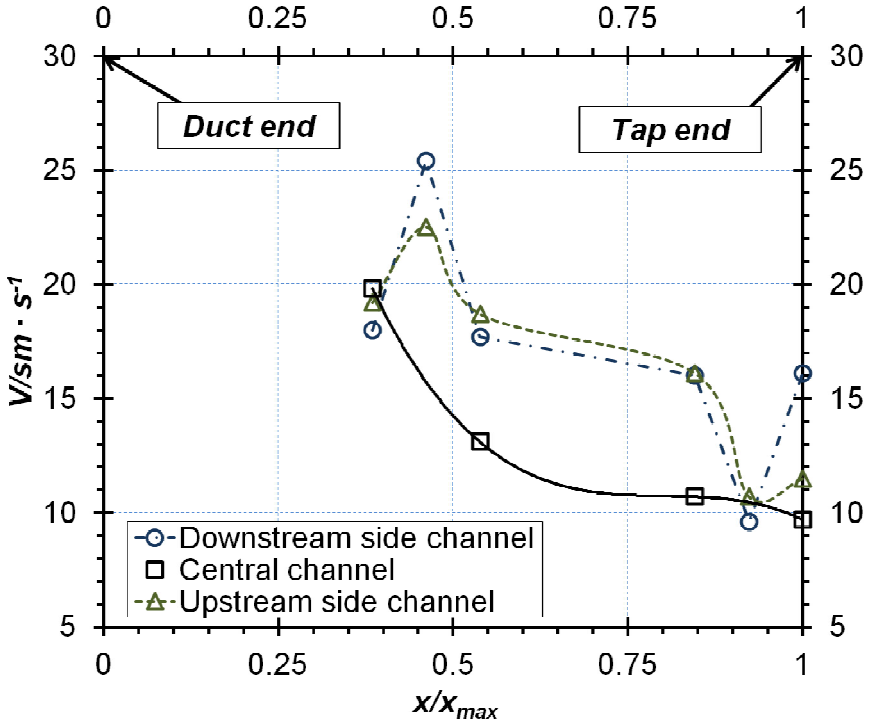

Fig. 4 – Dependence between the average bath velocity and the relative coordinate for three channels: downstream (◯), central (□) and upstream (△). Here x is the coordinate along the channel; x_{max} is the distance between the duct end and the tap end.

Measurement of the bath velocity allows noting the following:

– the average bath velocity along the upstream side closer to the middle of the cell (12.8 cm/s) is lower than that at the end of the cell (20.1 cm/s);

– the opposite results are observed in the ledge-anode area of the downstream side of the cell, where the average bath velocity closer to the middle of the cell (20.3 cm/s) is higher than the average velocity near the end (13.9 cm/s);

– the average bath velocity in the central risers area (14.6 cm/s) is lower than that in the side risers area (17.6 cm/s);

– the average bath velocity in the central channel closer to the end of the cell (16.5 cm/s) is higher than that in the middle of the cell (13.9 cm / s);

– the zones between feeders 2 and 3, and between feeders 5 and 6 have high velocities;

– it is possible to mark the areas with low bath velocity (points 3-5, 3-7, 6-4) and the areas with high velocity (points 3-4, 6-5).

3 Conclusion

The presence of velocity gradients in the bath indicates possible stagnant zones. Due to the low concentration of alumina in the ACD, a low rate of oxidation of the individual zones of the anode is inevitable. A complex picture of gas-hydrodynamic and MHD convection requires further investigation.

Acknowledgements

The paper was written using the results, taken during the project 02.G25.31.0181 implementation as a part of complex projects realization program of high efficiency production development, approved by Russian Federation government regulation No. 218 from April the 9th, 2010.

The authors would like to thank Aleksey Fertikov, Timofey Bermeshev, Liya Haritonova, Sergey Chyurikov, Sergey Babich, Boris Popov, Svetlana Derikova, Aleksandr Bezrukih and Pavel Yuriev for their help in performing measurements.

References

1. Kryukovskiy V.A., Polyakov P.V., Tsyplakov A.M., Yagodzinskiy V.I. Study of alumina concentration fields in industrial cell bathes [In Russ]. Tsvetnye metally, Vol. 8, 1973. pp. 29-34.

2. Kryukovskiy V.A., Polyakov P.V., Abramov A.A., Mikhalitsyn N.S., Mozhaev V.M. Investigation of mass transfer in aluminium reduction cell [In Russ]. Metallurgy, 1977., pp. 66-69.

3. Burnakin V.V., Kryukovskiy V.A., Polyakov P.V., Tsyplakov A.M., Zlobin B.S. Investigation of gas generation dynamics in melts on large-scale set-up with horizontal anode [In Russ]. Izv. Vuzov: Tsvetnaya metallurgiya, 1973, Vol. 3 pp. 38-42.

4. Polyakov P.V., Mozhaev V.M., Burnakin V.V., Kryukovskiy V.A., Nikolaenko V. E. On carbon dioxide bubbles evolution at cryolite-alumina melts electrolysis [In Russ]. Izv. Vuzov: Tsvetnaya metallurgiya, 1979, Vol. 1. Issue 52 pp. 55-58.

5. Bagshaw A. S., Kuschel I., Taylor M. P., Tricklebank S. B., Welch B. J. Effect of Operating Conditions on the Dissolution of Primary and Secondary Alumina Powders in Electrolysis. Light Metals, 1985, pp. 649-659.

6. Thonstad J., Solheim A., Rolseth S., Skar. O. The dissolution of alumina in cryolite melts/ Light Metals, 1988.

7. Chesonic D. C., LaCamera A. F., The influence of gas-driven circulation on alumina distribution and interface motion in a Hall-Heroult cell. Light Metals, 1990, pp. 211-220.

8. Von Kaenel R., Antille I., Romerio M. V., Besson O. Impact of magnetohydradynamic and bubbles driving forces on the alumina concentration in the bath of an Hall-Heroult cell. Light Metals, 2013, pp. 585-590.

9. Kalgraf K., Torlep K. Sediment transport and dissolution in Hall-Heroult cells. Light Metals, 1985, pp. 455-464.

10. Zoric I., Thonstad J., Haaberg T., The influence on current distribution by initial shape and position of an anode and by the curvature of the aluminium in prebake aluminium cells. Light Metals, 1988. pp. 445-453.

11. Moxnes B., Solheim A., Liane M., Srinsas E., Halkjelsvik A. Improved cell operation by redistribution of the alumina feeding. Light Metals 2009, pp. 461-466.

12. Yang Y., Jao B., Liu X., Wang Zh., Shi Zh., Hu X., Tao W., Liu F., Yu J. Discussion on Alumina Dissolution and Difussion in Commercial Aluminium Reduction Cells. Light Metals, 2018. pp. 507-513.

13. Mikhalev Yu.G., Polyakov P.V., Yasinskiy A.S., Polyakov A.A. spikes generation on anode of aluminium reduction cell. Tsvetnye metally, 2018, №9, pp.43-48.

14. Yasinskiy, A.S., Polyakov, P.V., Voyshel, Y.V., Gilmanshina, T.R., Padamata, S.K. Sedimentation behavior of high-temperature concentrated colloidal suspension based on potassium cryolite. Journal of Dispersion Science and Technology, 2018 Vol. 39 (10), pp. 1492-1501.

15. Yasinskiy, A.S., Polyakov, P.V., Yushkova, O.V., Sigov, V.A. Spatial particle distribution during Stokes sedimentation of alumina in high temperature concentrated suspension-electrolyte for aluminium production. Tsvetnye Metally, 2018 Vol. 2, pp. 45-50.

16. Potočnik V. and Laroche F. Comparison of measured and calculated metal pad velocities for different prebake cell designs – Light Metals 2001 pp. 419-425.

17. Kobbeltvedt O. and Moxnes B. P. On the bath flow, alumina distribution and anode gas release in aluminium cells. Light Metals, 1997, pp. 369-376.

18. Yuqing Feng, Mark A. Cooksey, M. Philip Schwarz CFD modelling of alumina mixing in aluminium reduction cells. Light Metals 2010. pp. 455-460.

19. Mozhaev V.M., Polyakov P.V., Utkin E.N., Burnakin V.V., Kryukovskiy V.A. Determination of liquid fluxes velocities in interelectrode space of aluminium reduction cell (on model) [In Russ]. Tsvetnye metally, 1976, Vol.7, pp.31-34.